Stress and structure at the NiO/Ag(001) interface

A. Dhaka,[1] D. Sander,[1] H. L. Meyerheim,[1,*] K. Mohseni,[1] E. Soyka,[1] J. Kirschner,[1] W. A. Adeagbo,[2] G. Fischer,[2] A. Ernst,[1] and W. Hergert[2]

[1]*Max-Planck-Institut für Mikrostrukturphysik, Weinberg 2, D-06120 Halle, Germany*

[2]*Institut für Physik, Martin-Luther-Universität Halle-Wittenberg, D-06099 Halle, Germany*

(Received 14 September 2011; published 9 November 2011)

We present a combined stress and structural analysis of the growth of epitaxial NiO monolayers on Ag(001). Our experimental results indicate an unexpectedly complex interface formation, where a fraction of the first NiO monolayer (ML) is embedded into the Ag surface. This interface formation induces a tensile surface stress change. Subsequent deposition leads to a layer-by-layer growth of NiO up to 5 ML. Here, the average film stress is compressive −5.8 GPa, and it corresponds quantitatively to the misfit-induced stress. Our density functional calculations complement the experimental results by identifying the proper O-Ag bonding geometry in the ML regime from two indistinguishable options as provided by the analysis of surface x-ray diffraction data.

DOI: 10.1103/PhysRevB.84.195441 PACS number(s): 68.35.Ct, 68.43.Fg, 68.60.Bs, 71.15.Mb

I. INTRODUCTION

The fundamental property of nanoscale materials is that a large fraction of atoms resides in low-coordinated sites. Surfaces and interfaces represent one specific and widely investigated type of nanostructure in which atoms experience a sudden change in coordination and/or in chemical environment, both leading to significant modification of the chemical and physical properties. Well-known examples are the formation of surface reconstructions[1] and modified magnetic properties.[2] The structure of the interface is also decisive for film growth. The interaction of the deposited film material with the surface may lead to structural relaxations and peculiar bonding situations, which differ from those within the film and from that of the pristine surface. Thus, studies of the structural and physical properties at interfaces are relevant to advancing the understanding of interface formation on the atomic scale.

In the present study, we have chosen a seemingly simple system, NiO on Ag(001), which is characterized by a small lattice misfit η of $\eta = (a_{Ag} - a_{NiO})/a_{NiO} = -0.022$ ($a_{Ag} = 4.086$ Å, $a_{NiO} = 4.177$ Å).[3] All previous studies point to a considerable complexity of the interface formation. This is expected to have considerable impact on structure and stress at the interface, and this aspect is elucidated here.

Numerous studies have been carried out in the past to investigate growth and structure of NiO on Ag(001),[4–14] but the atomic structure at the *interface* has not been quantitatively determined yet. Similarly, a number of quantitative low-energy ion scattering (LEIS), x-ray photoelectron spectroscopy (XPS), and x-ray absorption spectroscopy (XAS) studies[6–10] have dealt with the analysis of the geometric structure of NiO films on Ag(001), but concentrated on the thickness range well above 1 monolayer (ML), leaving the first stages of interface formation unexplored.

The NiO growth morphology has been investigated by scanning tunneling microscopy (STM), which indicated a complex morphology, where it has been suggested that embedding of NiO into the Ag(001) surface needs to be considered in the submonolayer coverage regime.[4,5,11,12] These studies and low-energy electron diffraction (LEED) experiments reported a (2×1) LEED pattern for room temperature deposition up to about 1.5 monolayer (1 ML: 1.20×10^{15} Ni and O atoms per cm^2) coverage. At higher coverage a transformation to a (1 × 1) pattern was found.[9,10] Mild annealing at 470–570 K induces a (2 × 1)$\Longrightarrow$ (1×1) structural transformation in the low coverage regime.

In this study we complete the understanding of the interface formation between NiO and Ag(001) by presenting the results of a combined experimental and theoretical study. Our structural investigation of the interface by surface x-ray diffraction is complemented by interface stress measurements and by theoretical studies in the framework of density functional theory of the bonding details.

We have carried out combined stress, medium-energy electron diffraction (MEED), and surface x-ray diffraction (SXRD) measurements. SXRD is very well suited to the study of complex interfaces which often involve fractional layer occupancies, since the data can be analyzed using single scattering theory. Our experimental studies are complemented by first-principles calculations based on density functional theory. Our results indicate a partial embedding of the first ML NiO into the Ag surface,[4,5,12] which is accompanied by an initial tensile surface stress change. Ongoing deposition above 2 ML leads to layer-by-layer growth of NiO, which is characterized by a misfit-induced compressive film stress of order −5.8 GPa. The main characteristic of the NiO-Ag interface formation is the fractional embedding of the first NiO layer into the Ag surface, which goes in parallel with the formation of a rather short bond length of about 1.9 Å between the O atoms located on top of the Ag-substrate atoms

II. EXPERIMENTAL DETAILS

The Ag(001) substrate was cleaned under ultra high vacuum (UHV) conditions by Ar-ion bombardment (1.5 keV, $I_{sample} = 2\,\mu$A) and subsequent annealing at 650 K until no traces of impurities were detected by Auger electron spectroscopy, and a sharp 1 × 1 diffraction pattern was observed by LEED. Stress measurements were performed by the crystal curvature technique, where the stress-induced change of curvature of the 0.1 mm thin Ag(001) crystal (length: 13 mm, width: 2.5 mm) was measured by an optical two beam deflection setup.[15]

III. RESULTS AND DISCUSSIONS

A. Stress and structure of NiO monolayers

Figure 1 shows simultaneously taken MEED intensity and stress measurements during Ni deposition on Ag(001) in an O_2 atmosphere. At time zero, oxygen has been introduced into the chamber, which is accompanied by a tensile stress change of +0.7 N/m. With a delay of 250 s the Ni evaporator has been opened. With the onset of Ni deposition in O_2 a sharp decrease of the MEED intensity is observed, as identified in regime I, where a further tensile stress change of +0.6 N/m is observed. Ongoing Ni deposition in regime II leads to pronounced periodic oscillations of the MEED intensity with a period of 75 s, and a compressive stress change to −6 N/m is measured. At 640 s, the MEED intensity oscillations decrease in amplitude, and the slope of the stress curve levels off in regime III. After 1750 s the deposition of Ni is ended, and the oxygen partial pressure is turned off.

We extract three different growth regimes from the combined stress and MEED experiments. Our results of regime I are at variance with the formation of an epitaxially strained NiO film on top of Ag(001). If this were the case we would expect a MEED oscillation already for the first layer. Also the stress change should reflect the compressive misfit between NiO and Ag of $\eta = -0.022$, which would induce a compressive stress change of −1.21 N/m per ML.[16]

The absence of MEED oscillations and the positive stress change in regime I are ascribed to the formation of a peculiar NiO-Ag interface, which deviates from a simple layer-by-layer growth of NiO on Ag(001). As pointed out in the following SXRD and theory discussion, our results provide

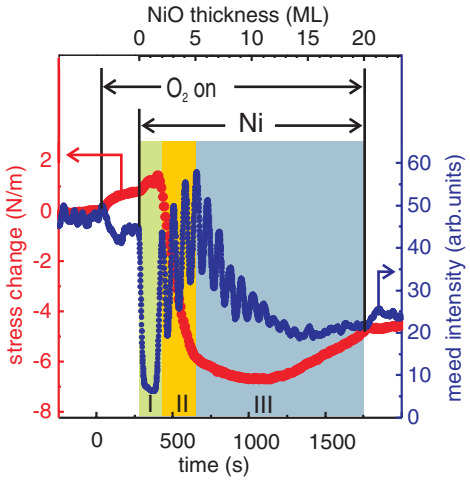

FIG. 1. (Color) Measured stress change (left scale) and MEED intensity (right scale) during Ni deposition on Ag(001) in an oxygen partial pressure of 2.0×10^{-7} mbar at 300 K. Pronounced MEED oscillations starting from 2 ML are ascribed to layer-by-layer growth of NiO. The compressive stress change from 2–5 ML NiO is due to epitaxial misfit between NiO and Ag. Three growth regimes are identified from the distinctly different stress and MEED observations. I (0–2 ML NiO equivalent): interface formation; II (2–5 ML NiO): pseudomorphic growth; and III (5–20 ML NiO): nonpseudomorphic growth. This assignment is corroborated by the SXRD data presented in Figs. 2 and 3, as explained in the text.

complementary support for the conjectures of earlier STM studies[4,5,12] on the embedding of NiO patches and the corresponding expelling of Ag atoms. Thus, misfit arguments fail to describe the stress change in regime I. Here, adsorbate-induced surface stress changes are more decisive than misfit stress.[15,17] Note that the exposure of the clean Ag surface to oxygen induces a tensile surface stress change (time 0–250 s in Fig. 1). Thus, we may tentatively ascribe the tensile stress change during the deposition of the first two ML NiO to the O-Ag interaction, which is expected from our structural analysis and calculations, as outlined below.

Stress and MEED results of regime II are attributed to layer-by-layer growth of strained NiO as reported previously.[14] The almost constant slope of the stress curve leads to a compressive stress change of −6 N/m at the end of regime II. This corresponds quantitatively to the calculated misfit stress for 5 ML NiO of −6.1 N/m. The leveling off of the stress curve and the decay of the MEED intensity oscillations in regime III are ascribed to a rougher film morphology and a reduced average film strain. We conclude that pseudomorphic growth ends at 5 ML NiO.

The stress measurements are complemented by SXRD measurements. They were carried out in an ultra-high-vacuum (UHV) diffractometer operated in the z-axis mode[18] using a rotating anode x-ray source (Cu-Kα radiation, $\lambda = 1.54$ Å) and a focusing multilayer monochromator.

Samples were prepared *in situ* by deposition of Ni by evaporation from a Ni rod heated by electron bombardment (thermal deposition, TD) at a rate of 0.23 ML per minute in an O_2 partial pressure of 2×10^{-7} mbar at 300 K followed by mild annealing up to 500 K to improve the long-range order as deduced by SXRD. The amount of NiO deposited was estimated by Auger electron spectroscopy (AES) and compared with SXRD showing good agreement. Integrated x-ray intensities (I_{obs}) were collected by rotating the sample about the surface normal under grazing incidence of the incoming beam. Structure factor amplitudes, $|F_{obs}| \propto \sqrt{I_{obs}}$, were derived by correcting the integrated intensities for instrumental factors.[18]

Each data set consists of 150–200 reflections along five crystal truncation rods (CTRs), reducing to about 120 independent reflections along four CTRs after averaging over symmetry equivalent reflections. Symbols in Fig. 2 represent on a log scale the experimental structure factor amplitudes, $|F|$, along the (10ℓ), (11ℓ), (20ℓ), and (21ℓ) CTR for samples where approximately 0.7, 1.9, and 3.1 ML NiO were deposited.

The CTRs arise due to the termination of the crystal,[19] therefore the coordinate ℓ of the normal momentum transfer $q_z = \ell \times c^\star$ becomes a continuous parameter [$c^\star = 1.53$ Å^{-1} is the reciprocal lattice unit (r.l.u.) of Ag along q_z]. Error bars represent the standard deviations (1σ) derived from the counting statistics and the reproducibility of symmetry equivalent reflections, and they indicate $\sigma \approx 5$–7%.

The total scattered structure factor F_{tot} is given by the interference between the structure factor of the semi-infinite Ag substrate F_{sub} and the contribution of the adsorbate atoms: $|F_{tot}| = |F_{sub} + F_{Ad} \exp[i\phi]|$, where the phase factor $\phi = 2\pi[hx + ky + \ell z]$ takes into account the registry of the

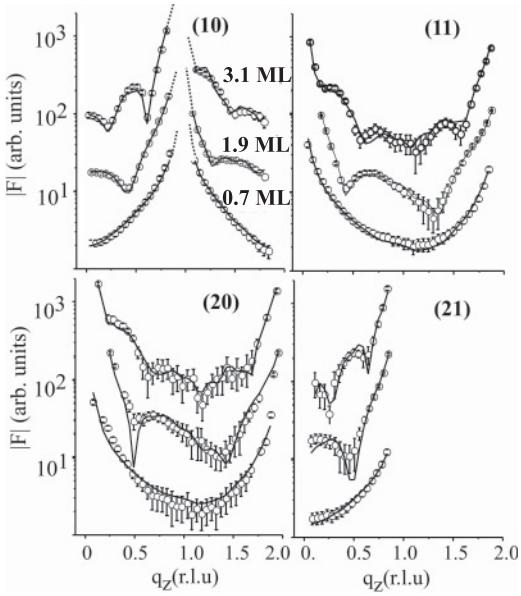

FIG. 2. Measured (symbols) and calculated (lines) structure factor amplitudes $|F|$ on a log scale along the (10ℓ), (11ℓ), (20ℓ), and (21ℓ) CTRs for samples with 0.7, 1.9, and 3.1 ML NiO.

adlayer. At the antiphase condition given by $h + k + \ell = 2n + 1$ (n = integer), the total scattered intensity of the bulk substrate crystal is equivalent to that of 1/4 of a Ag(001) ML: $I(hk\ell) \propto |\ F_{\text{sub}}\ |^2 = f_{\text{Ag}}^2/4$. It is the suppression of the substrate scattering contribution at positions in reciprocal space off the bulk Bragg-positions which makes the analysis "surface sensitive".

Inspection of Fig. 2 shows that with increasing coverage the overall shape of the CTRs changes from the U-shape profile characteristic of clean surfaces to an increasingly oscillating one with side maxima and minima depending on the number of layers. The quantitative analysis was carried out by least-squares refinement of the calculated $|\ F\ |$'s to the experimental ones using a program package based on the Prometheus software.[20]

Due to the high symmetry of the structure (plane group *p4mm*) modeling of the NiO structure requires one to consider only two independent atomic positions at (0,0,z) for Ni and (1/2, 1/2, z) for O, changing vice versa layer by layer. Therefore at most only two z parameters and one Debye parameter (B) representing disorder (static and dynamic) are necessary to characterize each layer. Within heterogeneous layers, different layer compositions are simulated by varying the site occupancy of NiO (Θ_{NiO}) and Ag (Θ_{Ag}). Since in the thickest film a maximum of five layers is sufficient to achieve fit convergence, at most 12–14 parameters including an overall scale factor are required to model the interface structure.

Solid lines represent the best fit to the data, whose quality is quantified by the unweighted residuum R_u and the goodness of fit (GOF) parameter.[21] We find values in the range between 7.8% and 12.3% for R_u and 1.24 and 1.88 for GOF, respectively. Visual inspection directly shows the high quality of the fits, where the calculated $|F|$'s follow the experimental ones in all details.

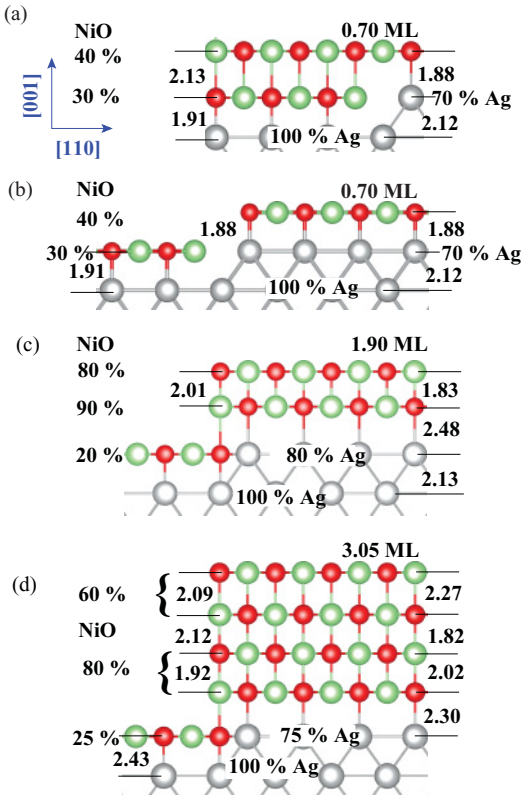

FIG. 3. (Color) Structure models for increasing NiO film thickness. Dark (small, red) and bright (mid-sized, green) spheres represent O and Ni atoms, respectively, Ag atoms are shown as large grey circles. Layer stoichiometry and interlayer spacings in Å are given.

Schematic structure models are shown in Fig. 3 for samples where 0.7, 1.9, and 3.05 ML of NiO were deposited. Green (mid-sized bright) and red (small, dark) spheres represent the Ni and O atoms, respectively, the largest grey spheres correspond to Ag atoms. For each layer, the fractional coverage in percent of a ML is indicated on the left, all distances are given in Å (standard deviation ≈0.07–0.15 Å). We estimate a ±1% uncertainty for the concentration determination, by keeping the Ni:O stoichiometry constant at 1:1.

The results of the structure analysis can be summarized as follows:

(i) The SXRD data clearly show that the NiO film coherently grows on the Ag(001) surface within the coverage regime investigated. We find a fraction of approximately 20–35% of a ML of NiO embedded into the first Ag layer. Oxygen atoms adsorb on top of the topmost Ag atoms, while Ni atoms reside in hollow sites. Embedding starts at the beginning of the growth and further deposition does not lead to a significant change of the concentration of embedded NiO [Figs. 3(c) and 3(d)]. The structure models shown in Figs. 3(a) and 3(b) represent two possible solutions, which cannot be distinguished by SXRD. In Fig. 3(a) the two NiO layers (occupancy 30% and 40%, respectively) are shown as a double layer, where the second layer directly grows above the first (embedded) one. In the second model [Fig. 3(b)] the top layer grows directly on the (upper) Ag(001) surface. The second model is generated by the first one by shifting the top layer by some unit cells

along the [110] direction. This has no effect on the x-ray intensities since by collecting integer order rods (h,k) lateral atomic shifts of a multiple of a unit cell $(\Delta x, \Delta y = 1)$ change ϕ by a multiple of 2π: $\Delta\phi = n \times 2\pi[h\Delta x + k\Delta y]$, with n integer. Our calculations indicate that the second model is more appropriate.

The structure models shown in Figs. 3(c) and 3(d) are in favorable agreement with previous STM studies[12] for comparable thickness regimes (coverage $\geqslant$1.5 ML) and preparation procedures.

Earlier STM studies[4,5] speculated that upon annealing, double-layer NiO patches form in the submonolayer coverage regime. The double-layer patches were proposed to grow on top of an embedded NiO island. This model was based on a comparison of the change of the areal density of NiO patches upon annealing. This conjecture of the earlier STM work seems to rule out our structural model presented in Fig. 3(b), but it agrees with the model of Fig. 3(a). However, recent STM studies by Rota *et al.*[13] examined the initial stage of growth of NiO on Ag(001), using atomic oxygen during deposition. The authors found that at the maximum coverage investigated (0.85 ML) NiO grows with a highly uniform monoatomic thickness.[13] Their findings are in perfect agreement with our structural model of Fig. 3(b).

In view of these STM results we are led to speculate that at the beginning of the NiO growth there might be a subtle dependence of the amount of NiO double layers formed on the detailed preparation procedure (e.g., temperature and duration of annealing, oxygen partial pressure, presence of atomic oxygen). The reliable identification of the atomic origin of voltage-dependent contrast is an inherent challenge of STM,[4] and this might explain why not all features, which are related to embedded single NiO layers, have been clearly identified by STM.

(ii) We find a distinct dependence of the vertical O-Ag distance $d_{\text{O-Ag}}$ on the film thickness. In the case where only one NiO layer is located on the Ag(001) surface, $d_{\text{O-Ag}}$ lies in the 1.80–1.90 Å range [0.7 ML sample, Figs. 3(a) and 3(b)]. By contrast, if a second NiO layer is grown, $d_{\text{O-Ag}}$ significantly increases by 0.3–0.4 Å finally reaching values as large as 2.3–2.5 Å for the 2 and 3 ML thick film [Figs. 3(c) and 3(d)]. As will be demonstrated on the basis of *ab initio* calculations, the evolution of $d_{\text{O-Ag}}$ can be attributed to the changing interface bond strength as a result of the back-bonding between the surface NiO layer and the layers of the growing film. Thus, the calculations identify that in the low coverage structure model shown in Figs. 3(a) and 3(b), the small value of $d_{\text{O-Ag}} = 1.91$ Å is not compatible with the presence of a second NiO layer on top of the first one. Rather, at this low coverage the calculations suggest that there exist two single layers on the metal surface (the lower one embedded; upper one on the surface, not embedded). Values $d_{\text{O-Ag}}$ determined for the 2 and 3 ML film (average: 2.403 Å) are in excellent agreement with values published previously for films of comparable thickness based on EXAFS ($d = 2.37 \pm 0.05$ Å)[6,7] and LEED ($d = 2.43 \pm 0.05$ Å).[9] Notably, for the related system CoO/Ag(001), a more recent quantitative LEED analysis of a 4 ML thick film derived very similar results.[22] There, an Ag-O interface bond length of 2.40 Å was found in perfect agreement with this study. In addition, the topmost interlayer spacing was reported to be expanded by at least +5.6% as compared to the bulk spacing (2.25 vs 2.13 Å, respectively), while the spacings between the deeper layer are almost bulklike. The comparison with the thickest film of our structural investigation, which is composed of four (incompletely covered) NiO layers [see Fig. 3(d)], indicates close similarities. We also find that the top NiO-interlayer spacing is larger than the deeper ones (average values: 2.18 vs 1.97 Å). However, the direct comparison between NiO and CoO needs to be treated with caution, because (a) CoO is reported not to be embedded into the Ag(001) surface, and (b) the LEED analysis does not take the complicated real structure into account. It is characterized by incomplete defective layers, which might also be a reason for the mediocre fit quality reported in Ref. 22.

(iii) Some rumpling within the NiO layers might be present, but it is within the experimental accuracy ($\approx$0.10 Å). The rumpling gives rise to different Ni-O interlayer distances (Ni-O and O-Ni) as shown in Fig. 3 on the left and right. As far as comparable with previous studies [2 ML sample in Fig. 3(c)] we find agreement in that oxygen atoms are located slightly ($\approx$0.05 Å) below the Ni atoms.[9] Some disagreement exists with regard to the Ni-O spacing for which we derive 1.83(7) Å vs 2.05(5) Å in Ref. 9. This comparison needs to be treated with caution, since samples in Ref. 9 have not been annealed, and subtle structural differences might result.

(iv) The average interlayer spacing of NiO shows a slight increase with increasing coverage (1.92 vs 2.04 Å for the 2 and 3 ML samples, respectively).

B. Density functional theory insights

To gain more insight into the experimental results, first-principles calculations based on density functional theory by means of the Vienna *ab initio* simulation package[23,24] have been performed. The NiO/Ag(001) system was approximated by finite slabs consisting of seven Ag layers for the substrate. A symmetric coverage by NiO is assumed. The slabs are separated by 14.50 Å vacuum. The ground-state magnetic AF II structure for NiO is assumed. Structural relaxations are taken into account and are considered to be converged if the forces on the atoms are less than 0.001 eV/Å.

Due to the strong correlations of the 3*d* electrons the general gradient approximation together with correlation corrections (GGA + U) is applied.[25] An on-site Coulomb energy $U =$ 7.3 eV and an exchange parameter $J = 1.0$ eV lead to a good representation of the bulk electronic properties and are used in all calculations. A cutoff energy for the plane-wave expansion of 400 eV and a Monkhorst-Pack $6 \times 6 \times 1$ k-point mesh guarantee the convergence of all slab calculations.

The NiO bulk lattice constant was calculated as $a_{\text{NiO}} =$ 4.19 Å. This overestimates the experimental value of 4.177 Å slightly by 0.3%. To correlate the theoretical work with the experimental setup, the theoretical lattice constant of 4.07 Å obtained for Ag has been used for the in-plane lattice constants of NiO and this value is kept fixed for both Ag and NiO during the relaxation in the z direction. The parameters correspond to a compressive misfit between NiO and Ag, $\eta = (a_{\text{Ag}} - a_{\text{NiO}})/a_{\text{NiO}} = -0.0286$, which is close to the experimental value of -0.022.

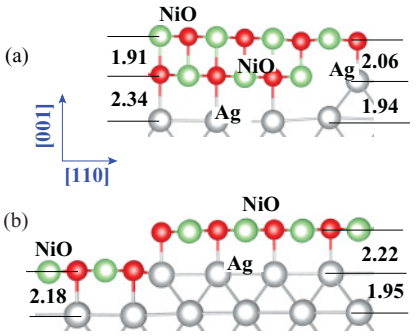

FIG. 4. (Color) Theoretical simulations of double NiO layer Ag(001) surface: (a) one NiO layer is embedded into the Ag(001) surface, another one is on top of the embedded NiO layer; (b) one NiO layer is embedded into the Ag(001) surface, another one is on the Ag(001) surface.

The calculations were carried out for the structural models derived from the SXRD experiment (see Fig. 3). As an example, we show in Fig. 4 the structural model for the lowest coverage film. The previously discussed two kinds of models are considered, namely, one with a NiO double layer (a), and one with two single layers, in which the first is embedded as in (a), while the second is located on the top Ag(001) terrace instead (b).

The most important result is that the interfacial O-Ag distance depends on whether there is a second (or more) NiO layer on top of the interfacial one. Theoretically derived distances for the two structure models are shown in Fig. 4. For $d_{\text{O-Ag}}$ spacing we find for the double-layer model $d_{\text{O-Ag}} = 2.34$ Å [see Fig. 4(a)], while for the two single-layer model [Fig. 4(b)] $d_{\text{O-Ag}} = 2.18$ and 2.22 Å is determined. The reduction of the O-Ag distances is due to missing back bonds to additional NiO layers in the single-layer model. Direct comparison with the experimental data shows that the low experimental value of $d_{\text{O-Ag}} \approx 1.9$ Å is not compatible with the presence of a NiO double layer, but rather with a two single-layer model, as has been discussed above, and is shown in Fig. 4(b).

Experimental values for $d_{\text{O-Ag}}$ are about 0.2–0.3 Å larger than the theoretical ones. This difference can be explained by two reasons:

(i) In a monolayer thin NiO film the correlation effects are not the same as in thicker films, but in our simulations the correlation parameter U was fixed to the bulk value. Some hint for this comes from the comparison between theory and experiment regarding the interlayer spacings between NiO layers in the case of thicker films, which agree to within 0.05 Å, well within the experimental uncertainty. They are also in very good agreement with other experiments and calculations for the same film thicknesses.[7,8,26]

(ii) In the experiment the NiO ML are partially occupied, which is not taken into account in our theoretical consideration. We may thus speculate that the onset of strong correlation effects requires a minimum of two NiO layers.

IV. CONCLUSIONS

Our combined experimental and theoretical investigation of the interface formation of NiO on Ag(001) reveals a complex growth mechanism. The NiO-Ag interface can be modeled by patches of NiO, embedded in the Ag surface, and by islands of NiO grown on top of the Ag surface. Approximately 30% of a ML is embedded in the surface, and the corresponding fraction of Ag atoms is expelled. A structural characteristic of this interface is a rather short Ni-O bond length of order 1.9 Å for the embedded NiO patch as compared to typical Ag-O distances in the range of 2.05 Å. The Ag-O distance increases with NiO deposition on top of the embedded NiO patch to 2.4 Å. We ascribe this bond length variation to the effect of back-bonding, which is absent at low coverage due to the lack of bonding partners. The unusually short Ag-O bond length relaxes in thicker films, where the structure is well described by an epitaxially strained NiO film. Stress measurements support this analysis. The interface formation is characterized by a tensile surface stress change, which can qualitatively be ascribed to the interaction between Ag and O. The epitaxial misfit determines the measured stress change only in thicker films beyond 2 ML. Thus, stress measurements identify different growth regimes from characteristic changes of the stress-coverage dependence. They provide quantitative values for interface and film stress, which may serve as benchmarks for future calculations.

ACKNOWLEDGMENT

This work is supported by the DFG through SFB 762.

*hmeyerhm@mpi-halle.mpg.de

[1]O. L. Alerhand, D. Vanderbilt, R. D. Meade, and J. D. Joannopoulos, Phys. Rev. Lett. **61**, 1973 (1988); R. D. Meade and D. Vanderbilt, *ibid.* **63**, 1404 (1989); K. Kern, H. Niehus, A. Schatz, P. Zeppenfeld, J. Goerge, and G. Comsa, *ibid.* **67**, 855 (1991); P. Zeppenfeld, M. Krzyzowski, C. Romainczyk, G. Comsa, and M. G. Lagally, *ibid.* **72**, 2737 (1994); H. Ibach, Surf. Sci. Rep. **29**, 193 (1997); **35**, 71 (1999) and references therein.

[2]D. Sander, W. Pan, S. Ouazi, J. Kirschner, W. Meyer, M. Krause, S. Müller, L. Hammer, and K. Heinz., Phys. Rev. Lett. **93**, 247203 (2004).

[3]*Crystal Data Determinative Tables, Vol. 2: Inorganic Compounds, 3rd ed.*, edited by J. D. H. Donnay and H. M. Ondik (National Standard Reference Data System (NSRDS), US Dept. of Commerce, Washington, 1973).

[4]Th. Bertrams and H. Neddermayer, J. Vac. Sci. Technol. B **14**, 1141 (1996).

[5]I. Sebastian, Th. Bertrams, K. Meinel, and H. Neddermayer, Faraday Discuss. **114**, 129 (1996).

[6]E. Groppo, C. Prestipino, C. Lamberti, P. Luches, C. Giovanardi, and F. Boscherini, J. Phys. Chem. B **107**, 4597 (2003).

[7]C. Lamberti, E. Groppo, C. Prestipino, S. Casassa, A. M. Ferrari, C. Pisani, C. Giovanardi, P. Luches, S. Valeri, and F. Boscherini, Phys. Rev. Lett. **91**, 046101 (2003).
[8]S. Casassa, A. M. Ferrari, M. Busso, and C. Pisani, J. Phys. Chem. B **106**, 12978 (2002).
[9]M. Caffio, B. Cortigiani, G. Rovida, A. Atrei, C. Giovanardi, A. di Bona, and S. Valeri, Surf. Sci. **531**, 368 (2003).
[10]M. Caffio, B. Cortigiani, G. Rovida, A. Atrei, and C. Giovanardi, J. Phys. Chem. B **108**, 9919 (2004).
[11]M. Caffio, A. Atrei, B. Cortigiani, and G. Rovida, J. Phys. Condens. Matter **18**, 2379 (2006).
[12]St. Großer, C. Hagendorf, H. Neddermeyer, and W. Widdra, Surf. Interface Anal. **40**, 1741 (2008).
[13]A. Rota, S. Altieri, and S. Valeri, Phys. Rev. B **79**, 161401 (2009).
[14]J. Wollschläger, D. Erdös, H. Goldbach, R. Höpken, and K. M. Schröder, Thin Solid Films **400**, 1 (2001).
[15]D. Sander, Z. Tian, and J. Kirschner, J. Phys. Condens. Matter **21**, 134015 (2009).
[16]We take the biaxial modulus of NiO $Y/(1-\nu) = 1/(s_{11}+s_{12}) =$ 263 GPa from the average of published values in *Landolt-Börnstein: Numerical Data and Functional Relationships in Science and Technology, New Series, Group 3*, Vol. 11 (Springer-Verlag, Berlin, 1979), p. 28. This gives a stress per ML of $\eta a_{\mathrm{NiO}} Y/[2(1-\nu)] = -1.21$ N/m.
[17]M. J. Harrison, D. P. Woodruff, J. Robinson, D. Sander, W. Pan, and J. Kirschner, Phys. Rev. B **74**, 165402 (2006).
[18]E. Vlieg, J. Appl. Crystallogr. **30**, 532 (1997).
[19]I. K. Robinson, Phys. Rev. B **33**, 3830 (1986).
[20]U. H. Zucker, E. Perenthaler, W. F. Kuhs, R. Bachmann, and H. Schulz, J. Appl. Crystallogr. **16**, 358 (1983).
[21]R. Feidenhans'l, Surf. Sci. Rep. **10**, 105 (1989).
[22]K.-M. Schindler, J. Wang, A. Chasse, H. Neddermeyer, and W. Widdra, Surf. Sci. **603**, 2658 (2009).
[23]G. Kresse and J. Hafner, Phys. Rev. B **47**, 558 (1993).
[24]G. Kresse and J. Furthmüller, Comput. Mater. Sci. **6**, 15 (1996).
[25]J. P. Perdew, J. A. Chevary, S. H. Vosko, K. A. Jackson, M. R. Pederson, D. J. Singh, and C. Fiolhais, Phys. Rev. B **46**, 6671 (1992).
[26]E. Groppo, C. Prestipino, C. Lamberti, R. Carboni, F. Boscherini, P. Luches, S. Valeri, and S. D'Addato, Phys. Rev. B **70**, 165408 (2004).